A Novel Attitude Estimation Algorithm Based on EKF-LSTM Fusion Model

Yufan Zhuo[1], Fuchun Sun[2], Zhenkun Wen[3], Huisi Wu[3], and Haiming Huang[1](✉)

[1] College of Electronics and Information Engineering, Shenzhen University, Shenzhen 518060, China
[2] Department of Computer Science and Technology, Tsinghua University, Beijing 100083, China
[3] College of Computer Science and Software Engineering, Shenzhen University, Shenzhen 518060, China

Abstract. The application of the low-cost inertial measurement unit (IMU) in many fields is growing, but the related attitude algorithms have the problems of low precision and poor adaptability. In this paper, a novel attitude estimation algorithm based on the fusion model of extend Kalman filter (EKF) and long short-term memory (LSTM) is proposed, which is composed of two main process: the initial attitude estimation of EKF and the subsequent calibration of LSTM. In this algorithm, EKF estimates the target's attitude angles by the inputs of sensor data from IMU, then LSTM makes a calibration of each axis' estimated angles, which is weighted with KEF's result to export the optimal estimation finally. The result of simulation experiment shows that this algorithm is 50.515% lower on average than EKF under different working conditions when using mean squared error (MSE) as the evaluation indicator, which could be concluded that this novel algorithm performs better than EKF, and provides a new way for attitude estimation.

Keywords: Attitude estimation · Extend kalman filter · LSTM · Neural network

1 Introduction

The low-cost, high-integration actuators and sensors are widely used in science and engineering with the rapid progressive technology of micro electro mechanical system (MEMS) [1]. Among these devices, a large number of applications of the inertial measurement unit (IMU) [2] integrated with the gyroscope, the accelerometer and the magnetometer are adopted widely in many fields such as robotic controlling, navigation system and kinesiology. While using the low-cost IMUs for the target's attitude estimation, some flaws will show up. For example, long term use of gyroscope will generate an integral accumulation error due to its temperature drift characteristic, the accelerometer and the magnetometer are easily affected by vibration and electromagnetic perturbations. Gaining the optimal estimation of the target's posture changes with the data fusion of acceleration, angle velocity, magnetic field and other sensors' data is an important orientation of attitude algorithm [3].

F. Sun et al. (Eds.): ICCSIP 2020, CCIS 1397, pp. 94–104, 2021.
https://doi.org/10.1007/978-981-16-2336-3_8

There is a great diversity of algorithms applied for attitude estimation, such as Kalman filter [4–6], complementary filter [7, 8], the fusion of these two algorithms [9, 10], and neural network [11, 12] in machine learning. Complementary filter is simply calculated but with low precision. Kalman filter has the problem of modeling deviation and the equilibrium between the accuracy and the computation of iterations. Furthermore, these traditional methods need the mathematical model of the target system which is usually a nonlinear system, and the actual ambient noise is not conformed to the condition of Gaussian distribution.

Artificial neural network (ANN) uses numbers of data processing units to simulate the neural network structure of the biological brain, which has good nonlinear mapping capability and adaptive ability [13]. As an important branch of ANN, the recurrent neural network (RNN) is widely used to semantic recognition and content recommendation due to its ability to establish a connection between current data processing and previous information with the long data sequence of time-domain sampling. However, RNN easily reaches the past best value with the problem of gradient dispersion and explosion. Long short-term memory (LSTM) network solves the problem of gradient disappearance through structural improvement [14]. LSTM takes advantage of a cell state link to transmit correlation of input's data, which has more advantages in processing longer time series data, and it is widely used combined with traditional algorithms such as self-model improvement [15], pose regularization [14].

The sensor sampling data of IMU are long time series sequences with a high temporal correlation between the front and rear frames. In this paper, an EKF-LSTM fusion model are proposed which uses LSTM to calibrate the outputs of EKF's attitude estimation, and it compensates the EKF's modeling deviation and reduces the influence of external disturbance to the optimal estimate.

The rest of the article is framed as follows: Sect. 2 explains the EKF's attitude estimation and introduces the LSTM general principle, then an EKF-LSTM fusion model for attitude estimation is described. Section 3 preforms the simulation experiment and the analysis of result. Conclusion is expounded in Sect. 4.

2 Related Background

The novel attitude estimation algorithm consisted of EKF and LSTM is a fusion algorithm, in which EKF makes the target's initial estimation based on the sensor data of IMU, then LSTM calibrates the EKF's result with the temporal context of sensor data to expert the optimal estimation of attitude angles.

2.1 Extended Kalman Filter

Extended Kalman filter is the extension of Kalman filter under the situation of nonlinear dynamic modeling. Extended Kalman filter could be considered an iterative self-feedback circulation, which principally consist of the prediction phase and the update phase [16].

In the prediction phase, extended Kalman filter base on the last time step's updated system state to predict the current state's mean $\hat{x}_k'$ and covariance $\hat{P}_k'$:

$$\hat{x}_k' = f\left(\hat{x}_{k-1}, u_k\right) \tag{1}$$

$$\hat{P}_k' = F\hat{P}_{k-1}F^T + Q \tag{2}$$

In the update phase, extended Kalman filter uses $\hat{P}_k'$ in Eq. 2 to calculate the Kalman gain K_k, and update the mean and the covariance of current state with the system current observable measurement z_k:

$$K_k = \hat{P}_k' H^T \left(H\hat{P}_k' H^T + R\right)^{-1} \tag{3}$$

$$\hat{x}_k = \hat{x}_k' + K_k\left(z_k - h\left(\hat{x}_k'\right)\right) \tag{4}$$

$$\hat{P}_k = (I - K_k H)\hat{P}_k' \tag{5}$$

For the dynamic modeling of attitude estimation, the usual way is linearizing the state transition equation f via Taylor series expansion. We adopt the quaternion q to explain rotation between the carrier coordinate system b and the geographical reference coordinate system n. The rotator from n to b could declare as:

$$q = \cos\tfrac{\theta}{2} + u^R \sin\tfrac{\theta}{2} \tag{6}$$

where u^R are the instantaneous axis and the direction of rotation, θ is the rotation angle.

In Eq. 1, the state transition equation f could be the quaternion differential equations of Picard algorithm in first approximation, and the state transition matrix F in Eq. 2 is the Jacobian matrix of f. So, the state's mean prediction function of extend Kalman filter could explained in matrix form, where $\hat{x}$ is the quaternion and u is the current state's 3-axis gyro data w_x, w_y, w_z:

$$\begin{bmatrix} q_0 \\ q_1 \\ q_2 \\ q_3 \end{bmatrix}_k = \left(I + \frac{dt}{2}\begin{bmatrix} 0 & -w_x & -w_y & -w_z \\ w_x & 0 & w_z & -w_y \\ w_y & -w_z & 0 & w_x \\ w_z & w_y & -w_x & 0 \end{bmatrix}\right) * \begin{bmatrix} q_0 \\ q_1 \\ q_2 \\ q_3 \end{bmatrix}_{k-1} \tag{7}$$

The measurement function h in Eq. 2 transform the quaternion into the dimension of z_k in b which is consisted of 3-axis accelerometer and 3-axis magnetometer. The acceleration of gravity in n always be one G of z-axis, in order to align it at the dimension of the accelerometer in b, the rotation matrix R_n^b multiplies by the optimal gravity matrix to get the projection of gravity in b. Meanwhile, magnetic field intensity in n always have the components of geographic north and verticality under the north east astronomical coordinate system, in order to get the projection of magnetic field distribution on b, the magnetic field distribution n_x, n_z on n could be calculated by the rotation matrix R_b^n and the magnetometer's 3-axis data m_x, m_y, m_z, then the projection of magnetic field distribution on b could be gained by n_x, n_z and R_n^b. So the measurement function h is given by:

$$h\left(\hat{x}_k^{'}\right) = \begin{bmatrix} 2(q_1q_3 - q_0q_2) \\ 2(q_2q_3 + q_0q_1) \\ q_0^2 - q_1^2 - q_2^2 + q_3^2 \\ n_x\left(q_0^2 + q_1^2 - q_2^2 - q_3^2\right) + 2n_z(q_1q_3 - q_0q_2) \\ 2n_x(q_1q_2 - q_0q_3) - 2n_z(q_2q_3 + q_0q_1) \\ 2n_x(q_1q_3 + q_0q_2) + n_z\left(q_0^2 - q_1^2 - q_2^2 + q_3^2\right) \end{bmatrix} \tag{8}$$

In Eq. 3 and 5, the measurement matrix H is the Jacobian matrix of h. In order to gain the Euler angles from EKF, we use the transformation between Euler angles and quaternion that is calculated as:

$$\emptyset = \tan^{-1}\left(\frac{2(q_1q_2+q_0q_3)}{q_0^2+q_1^2-q_2^2-q_3^2}\right) \tag{9.1}$$

$$\theta = \sin^{-1}(-2(q_0q_2 + q_1q_3)) \tag{9.2}$$

$$\varphi = \tan^{-1}\left(\frac{2(q_0q_1+q_2q_3)}{q_0^2+q_1^2-q_2^2-q_3^2}\right) \tag{9.3}$$

where $\emptyset$, θ, φ are the representations of the pitch, yaw and roll [17].

2.2 Long Short-Term Memory

As the improved part of recurrent neural network (RNN), Long short-term memory neural network (LSTM NN) is superior than RNN with the solution of vanishing gradient problem. With regard to the time domain continuously sampled data from IMU, LSTM have an advantage on processing these sensor data because of its time memory function. As shown in Fig. 1, each LSTM network unit has three correlative gates and a state of cells h. The forget gate determine discarded information of the state of cells h_{t-1} by the current input x_t and the last output y_{t-1}, which activation function always is logarithmic logical curves [18]. The input gate adds new information into the state of cells h_t. The final process is the output gate, which control the structure of LSTM's output y_t. The activation functions of the input gate and output gate of units are usually hyperbolic tangent curves [19, 20]. The state of cells containing all the time node information is the crucial part of LSTM structure, which will transmit on the cells' wiring with a few linear operations.

2.3 EKF-LSTM Fusion Model for Attitude Estimation

The EKF-LSTM fusion model for attitude estimation is shown in the Fig. 2. In the scheme, the inputs of model are consisted of the IMU's sensor data (ACC, GYRO, MAG) from the current moment. Firstly EKF makes the initial attitude estimation of target's 3-axis Euler angles (roll, pitch, yaw) through the prediction phase and the update

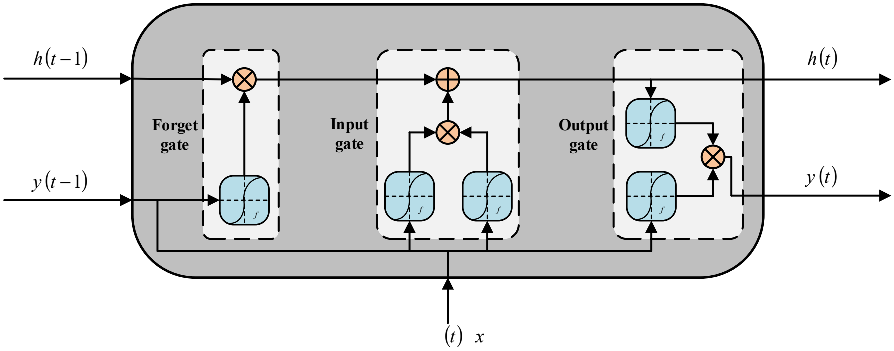

Fig. 1. The structure of the LSTM unit

phase. Then the EKF's results and the original sensor data are fitted into three LSTMs instead of one LSTM to avoid the cross coupling [21], where each LSTM adjusts EKF's attitude estimation in a small range according to the potential relationship between sensor data and the outputs of LSTM are each attitude angles' calibration. Finally, model's outputs are the calibrated attitude Angles, which are combined of the results of EKF and LSTMs. The model's framework takes EKF as the core, takes LSTM as the bias calibrator of EKF's nonlinear fitting, and its final output is the optimal estimate of 3-axis attitude angles.

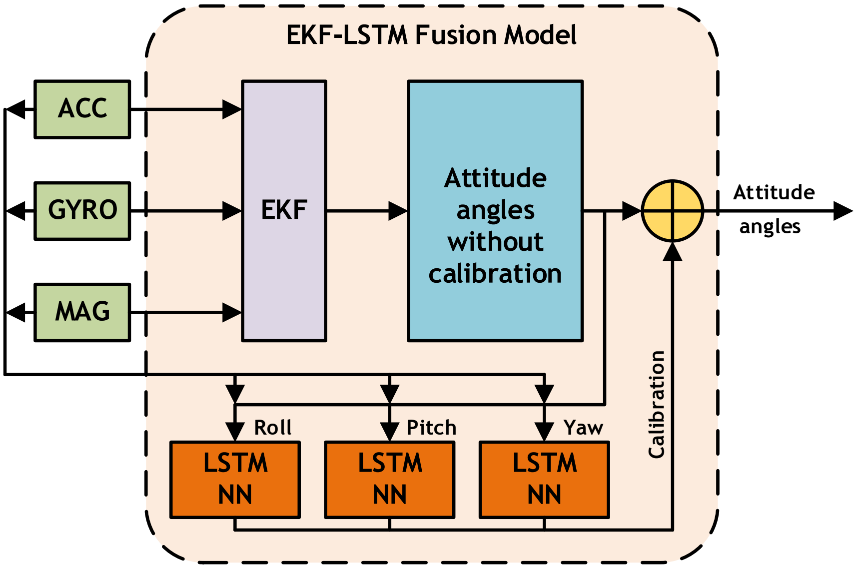

Fig. 2. The scheme of EKF-LSTM fusion model

The mean squared error (MSE) is used to evaluate model's output performance, the smaller MSE, the higher accuracy of the model, the equation of MSE as:

$$MSE = \frac{1}{N}\sum_{i=1}^{n}(\overline{m}_i - m_i)^2 \tag{10}$$

where $\overline{m}_i$ is the model's output, m_i is the true value.

3 Simulation Experiment and Analysis

In order to test the EKF-LSTM fusion model in Sect. 2, the simulation experiment bases on the deep learning framework using Python 3.6 and Keras 2.2.4. The experiment's computer is configured as: Intel Core i5 -8250U 1.60 GHz, 8 GB RAM. The experiment's IMU is JY901 which is integrated with accelerometer, gyroscope and magnetometer to obtain the sensor data and actual Euler angles in various conditions with the sampling rate of 200 Hz.

Figure 3 shows the sensor data of 3-axis gyroscope, 3-axis accelerometer, 3-axis magnetometer, which are almost 6000 training data. The first 4500 points of data are selected to train the EKF-LSTM fusion model and the LSTM as the contrast, and the rest data are selected to validate the model.

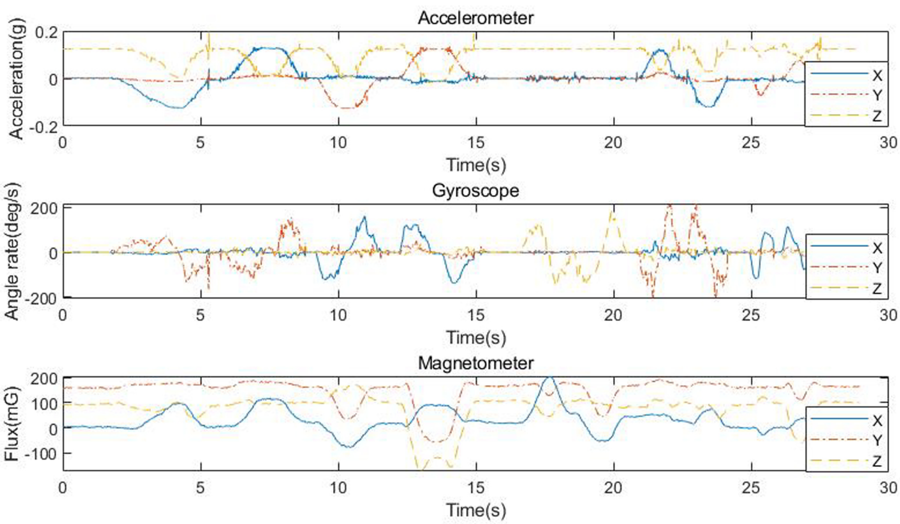

Fig. 3. The sensor data sampling from IMU

Firstly, the separate EKF is used to estimate the attitude Angle of the three axes to determine its estimated performance. In Fig. 4, the attitude estimation of EKF is closed to the true value in terms of roll and pitch, where is only a slight deviation during drastic angle changes, but the estimation of yaw has a obvious deviation because of EKF's nonlinear fitting deviation. EKF's MSE in roll, pitch and yaw are 0.00218, 0.00197 and 0.04931.

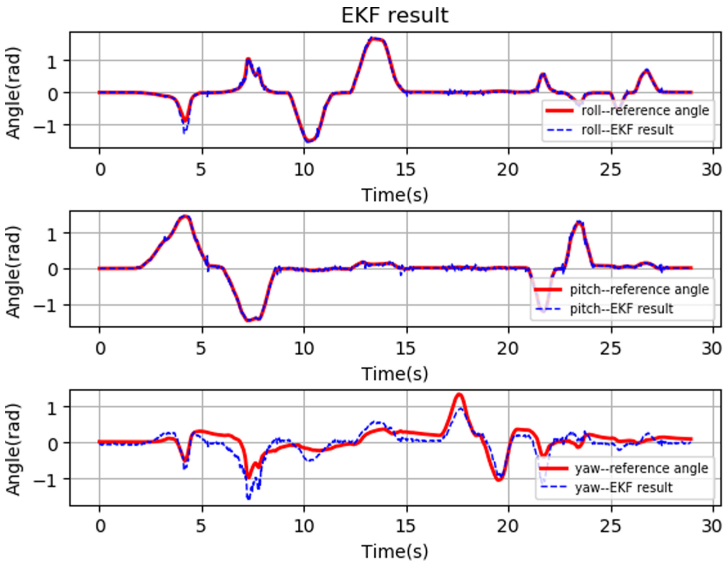

Fig. 4. The Euler angles of EKF result

Secondly, in order to achieve the optimal calibration effect of LSTM, the selecting of interior parameters should be confirmed by comparative experiment. In the LSTM parameters comparison experiment, the parameters such as the numbers of neurons in the hidden layer (HN), the timesteps (TS), the training time (TT), the MSE of roll (MSE1), the MSE of pitch (MSE2) and the MSE of yaw (MSE3) are listed in Table 1. It could be figured out that the MSEs decrease gradually as HN increases but MSEs begin to increase as HN exceeds a certain value. As TS increases, the MSEs decrease gradually but TT has a sharp increase simultaneously. Considering the accuracy and real-time performance of the algorithm, the parameters of No. 5 is adopted.

Table 1. The parameters and comparative results of LSTM parameters selecting experiment.

No	HN	TS	Epoch	TT(s)	MSE1	MSE2	MSE3
1	10	2	40	46.24	0.00082059	0.00066379	0.0077
2	10	5	40	73.57	0.00075836	0.00056065	0.0066
3	10	10	40	119.51	0.00062646	0.00050121	0.0048
4	20	2	40	46.01	0.00078448	0.00063158	0.007
5	20	5	40	76.98	0.00061906	0.00053342	0.005
6	20	10	40	120.5	0.0004358	0.00034101	0.0028
7	30	2	40	46.81	0.00084767	0.00062017	0.0072
8	30	5	40	77.31	0.00052815	0.00052687	0.0048
9	30	10	40	122.78	0.00032836	0.0002953	0.0021

Finally, as shown in Fig. 5, the validation of EKF-LSTM fusion model has better fitting quality especially in yaw comparing the EKF's result. The MSE of roll, pitch and yaw are 0.00049, 0.00119 and 0.02386.

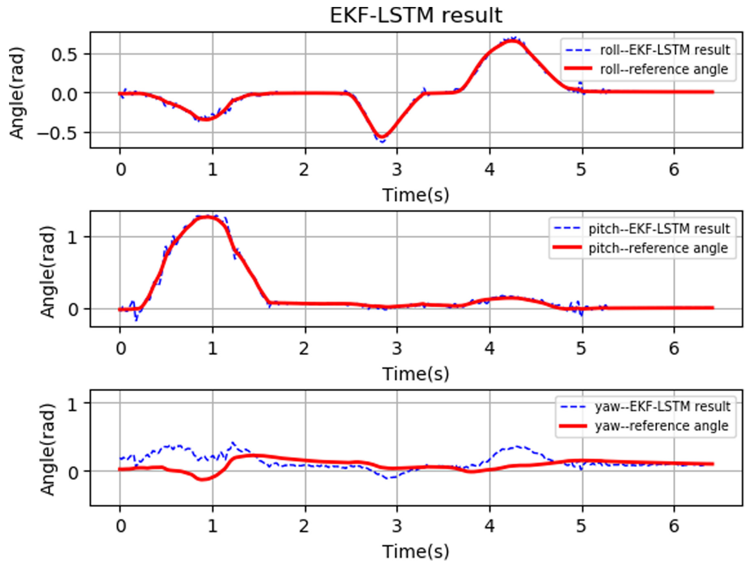

Fig. 5. The Euler angles of EKF-LSTM test result

By comparing the result of MSE between the EKF and the EKF-LSTM fusion model, EKF-LSTM has an improvement on estimation accuracy, which is 56.24% lower on average than EKF in MSE. In order to evaluate the adaption of EKF-LSTM on various working condition, the sensor data with the vibration and electromagnetic interference are collected to test its adaptive capacity.

As shown in Fig. 6 and Fig. 7, the result of EKF reflects that the fluctuation in a small range is relatively frequent in each axis. However, the result of EKF-LSTM fusion model shows that its curves are smoother with fewer destabilization.

As shown in Fig. 8, the errors of EKF-LSTM fusion model in roll and pitch are lower and more stable than EKF's, but the error between these two models in yaw are both in a great fluctuation which means that the calibration is out of work caused by the major estimation deviation of EKF. The EKF's MSE of roll, pitch and yaw are 0.00972, 0.01079 and 0.01731, correspondingly the EKF-LSTM's MSE of roll, pitch and yaw are 0.000237, 0.00095 and 0.02674, which is 44.79% lower on average than EKF.

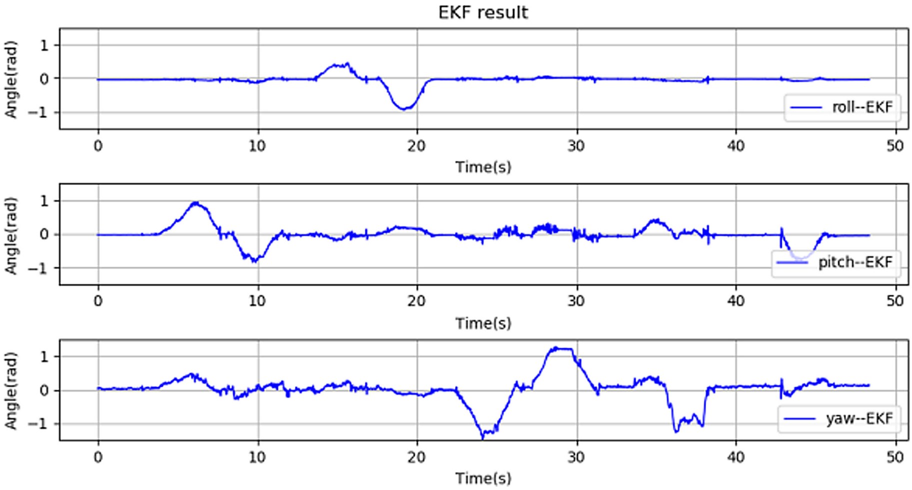

Fig. 6. The Euler angle of EKF result with electromagnetic interference

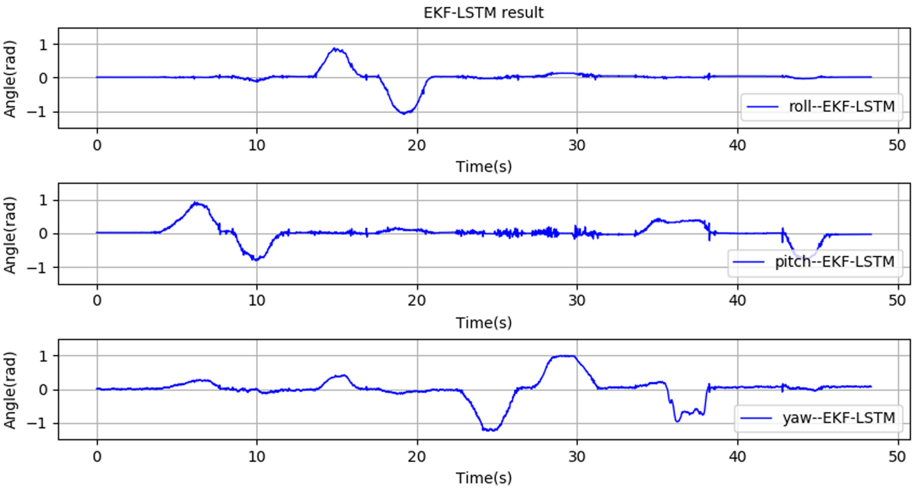

Fig. 7. The Euler angle of EKF-LSTM result with electromagnetic interference

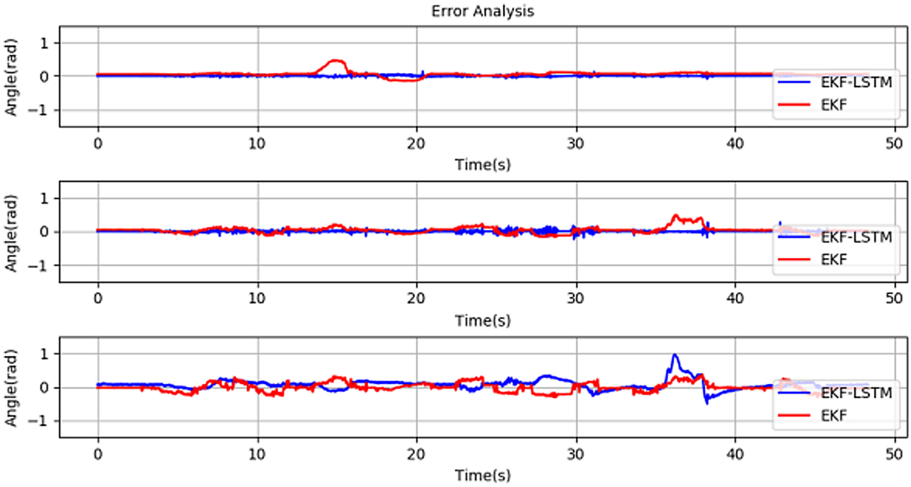

Fig. 8. The error analysis between EKF and EKF-LSTM

4 Conclusion

In this paper, a novel attitude estimation algorithm based on EKF-LSTM fusion model is proposed, which is consisted of EKF's initial attitude estimation and LSTM's Euler angles calibration. When taking MSE as the evaluation criterion, this algorithm is 50.515% lower on average than the traditional attitude estimation algorithm EKF under different working conditions, which explains that this novel algorithm has an improvement on accuracy and adaptability. The EKF-LSTM fusion model is proposed based on the LSTM's advantage of time sequential data processing and the traditional algorithm's problem of the modeling deviation and poor adaptability, which has some downsides that the algorithm verification experiment and multi-algorithm comparison experiment under different working conditions still need to be improved. In the future's research, this algorithm will be improved by using LSTM to adjust EKF internal parameters in real time to improve the adaptability, and physical verification experiments will be conducted, such as attitude calculation for unmanned aerial vehicle, manual motion acquisition and so on.

Acknowledgement. The authors are grateful for the support by the National Natural Science Foundation of China (Nos. 61803267 and 61572328), the China Postdoctoral Science Foundation (No. 2017M622757), the Beijing Science and Technology program (No. Z171100000817007), and the National Science Foundation (DFG) in the project Cross Modal Learning, NSFC 61621136008/DFG TRR-169. The authors are grateful for the support of Science and Technology Commissioned Project scheme of Shenzhen University.

References

1. Khoshnoud, F.: Recent advances in MEMS sensor technology-mechanical applications. Instrum. Measur. Mag. **15**(2), 14–24 (2012)

2. Kuang, J., Niu, X., Chen, X.: Robust pedestrian dead reckoning based on MEMS-IMU for smartphones. Sensors-Basel **18**(5), 1391 (2018)
3. Pierleoni, P., Belli, A., Palma, L., Pernini, L., Valenti, S.: An accurate device for real-time altitude estimation using data fusion algorithms. In: IEEE/ASME International Conference on Mechatronic & Embedded Systems & Applications, 2014 (2014)
4. Hajiyev, C., Conguroglu, E.S.: Integration of algebraic method and EKF for attitude determination of small information satellites. In: 7th International Conference on Recent Advances in Space Technologies (RAST), 2015 (2015)
5. Markley, F.L., Sedlak, J.E.: Kalman filter for spinning spacecraft attitude estimation. J. Guidance Control Dyn. **31**(6), 1750–1760 (2015)
6. Li, H., Tang, Q., Li, J.: Attitude/position estimation of monocular vision based on multiple model Kalman filter (2018)
7. Vlastos, P., Elkaim, G., Curry, R.: Low-cost validation for complementary filter-based AHRS. In: 2020 IEEE/ION Position, Location and Navigation Symposium (PLANS) (2020)
8. Del Rosario, M.B., Lovell, N.H., Redmond, S.J.: Quaternion-based complementary filter for attitude determination of a smartphone. IEEE Sens. J. **16**(15), 6008–6017 (2016)
9. Chen, M., Xie, Y., Chen, Y.: Attitude estimation of MEMS based on improved quaternion complementary filter. J. Electron. Measur. Instrum. **29**(9), 1391–1397 (2015)
10. Zhang, D., Jiao, S.M., Liu, Y.Q.: Fused attitude estimation algorithm based on complementary filtering and Kalman filtering. Transducer Microsyst. Technol. **36**, 62–66 (2017)
11. Du, S., Wu, H., Zhang, J., Ma, W.: Kind of improving compensation filter algorithm for AHRS. Foreign Electron. Measur. Technol. **3**, 13–18 (2015)
12. Omid, D., Mojtaba, T., Raghvendar, C.V.: IMU-based gait recognition using convolutional neural networks and multi-sensor fusion. Sensors-Basel **17**(12), 2735 (2017)
13. Jain, A., Zamir, A.R., Savarese, S., Saxena, A.: Structural-RNN: deep learning on spatio-temporal graphs. In: Computer Vision & Pattern Recognition, 2016 (2016)
14. Coskun, H., Achilles, F., Dipietro, R., Navab, N., Tombari, F.: Long short-term memory kalman filters: recurrent neural estimators for pose regularization. In: 2017 IEEE International Conference on Computer Vision (ICCV), 2017. IEEE (2017)
15. Wang, J.J., Wang, J., Sinclair, D., Watts, L.: A neural network and Kalman filter hybrid approach for GPS/INS integration. In: 12th IAIN Congress and 2006 International Symposium (2006)
16. Wang, J., Ma, J.: Research on attitude algorithm of EKF and complementary filtering fusion. Chin. J. Sens. Actuators **31**(8), 1187–1191 (2018)
17. Nonami, K., Kendoul, F., Suzuki, S., Wei, W., Nakazawa, D.: Autonomous Flying Robots. Springer, Japan (2010). https://doi.org/10.1007/978-4-431-53856-1
18. Karim, F., Majumdar, S., Darabi, H., Chen, S.: LSTM fully convolutional networks for time series classification. IEEE Access **6**(99), 1662–1669 (2018)
19. Yildirim, Z.: A novel wavelet sequences based on deep bidirectional LSTM network model for ECG signal classification. Comput. Biol. Med. **96**, 189–202 (2018)
20. Liu, J., Wang, G., Duan, L.Y., Abdiyeva, K., Kot, A.C.: Skeleton-based human action recognition with global context-aware attention LSTM networks. IEEE Trans. Image Process. **27**(99), 1586–1599 (2018)
21. Qu, D.C., Feng, Y.G., Fan, S.L., Qi, C.: Study of a fault diagnosis method based on Elman neural network and trouble dictionary (2008)